A Broadband Microstrip Array Antenna for 3G Smart Antenna System Testbed

Zainol Abidin Abdul Rashid, Mohammad Tariqul Islam, Ng Kok Jiunn
Faculty of Engineering, Department of Electrical, Electronics and System Engineering
Universiti Kebangsaan Malaysia
Email: zaar@vlsi.eng.ukm.my, titareq@yahoo.com

Abstract

A compact and broadband 4×1 array antenna was developed for 3G smart antenna system testbed. The 4×1 uniform linear array antenna was designed to operate at 1.885 to 2.2GHz with a total bandwidth of 315MHz. The array elements were based on the novel broadband L-probe fed inverted hybrid E-H (LIEH) shaped microstrip patch, which offers 22% size reduction to the conventional rectangular microstrip patch antenna. For steering the antenna beam, a commercial variable attenuator (KAT1D04SA002), a variable phase shifter (KPH350SC00) with four units each, and the corporate 4-ways Wilkinson power divider which was fabricated in-house were integrated to form the beamforming feed network. The developed antenna has an impedance bandwidth of 17.32% (VSWR≤1.5), 21.78% (VSWR≤2) with respect to center frequency 2.02GHz and with an achievable gain of 11.9dBi. The design antenna offer a broadband, compact and mobile solution for a 3G smart antenna testbed to fully characterized the IMT-2000 radio specifications and system performances.

Keywords: Array, feed network; dual parallel slots; E-H shaped patch antenna; microstrip antenna; L-probe fed.

1. INTRODUCTION

Recently, there has been a great effort to build smart antenna systems to meet the ever demanding channel capacity for the future generation broadband mobile third generation (3G) communication systems [1-3]. Smart antenna has been proposed by the ITU IMT-2000 as one of the key component to meet the current and future demands of the 3G mobile wireless network. A smart antenna system basically comprises a number of antenna elements or antenna array arranged in various configurations (linear, circular or planar) and a beamforming network which consists of amplitude and phase control network that provides the appropriate weight vectors which gives the ability of the antenna to form its beam to the intended user. The beamforming network can be implemented in either RF circuitry, real-time digital signal processing hardware, or in a hybrid solution.

Apart from the many research and development (R&D) programme on smart antenna system (SAS) worldwide, three non-commercial programmes have been actively promoting and advancing the research in this area. These are; the European TSUNAMI programme, the Circuit and System Group programme of the Uppsala University, and the MPRG (mobile and portable

radio group) programme of the Virginia Tech. University. These programmes have developed their own smart antenna testbed for the study and performance evaluation of smart antenna system for 3G wireless networks.

The antenna system of the smart antenna testbed of the TSUNAMI programme is based on a vertically polarized eight elements dipole array at the base station [4], while the Uppsala programme is based on a ten element patch antennas in circular arrangement [5], and the MPRG programme (MPRG antenna array testbed (MAAT)) is based on eight element antenna array of a quarter wavelength monopoles configured either in uniform linear or circular array [6]. These testbeds, apart from employing narrowband antennas, are somewhat simple, bulky, and difficult to move around but, nevertheless, are sufficed for the evaluation of smart antenna system.

To properly characterize the IMT-2000 or 3G radio specifications, a true broadband smart antenna testbed that cover the IMT-2000 band (1.88 – 2.2 GHz) is required. This paper discusses the design and the development of a broadband antenna array and a simple smart antenna testbed for 3G base station. The broadband capability of the antenna array is obtained by using our novel broadband and compact LIEH microstrip patch antenna. In this paper, in Section 2, we first gives a brief review on the state-of-the-art of microstrip broadband techniques before discussing on the design of the novel LIEH broadband microstrip element. Later in Section 3, we give the design and development of a broadband antenna array for 3G smart antenna system based on LIEH microstrip patch antenna. In Section 4 we present the results and finally in Section 5 we concluded the paper.

2. LIEH PATCH ELEMENT DESIGN

Recently microstrip patch antennas and arrays have been given great attention for the development of smart antenna system due to their various advantages including low profile, lightweight, easy fabrication and conformability to mounting structure. Much of the current researches on microstrip patch antennas are concentrated on broadband techniques [7-9] to meet the current broadband applications and on printed array and feeding techniques [10-11].

One of the widely used techniques for microstrip broadband is to embed a U-slot on a rectangular patch antenna, hence U-slot patch. This technique has achieved an impedance bandwidth of around 10-40% by employing various fabrication techniques such as the used of foam, air, and a mixture of these [7-9]. However this design does not permit fabrication of integrated circuit on the conducting patch presenting a serious disadvantage for an array antenna development. The E-shaped patch is the extension of the U-slot patch which incorporates two parallel slots on a rectangular patch antenna is simple to construct and can achieve an impedance bandwidth of better than 30%. The introduction of an inverted U-slot or E-slot patch with the PCB dielectric serving as a superstrate allows the patch to be designed and fabricated by integrated circuit technique [12]. Further, the superstrate can serve as the protective cover for the patch. Major problems to these design is the inherently high crosspolarization level on the H-plane.

The following subsection discusses the design of antenna element using the novel inverted hybrid E-H microstrip patch element with comparable broadband impedance bandwidth to the U- or E-slot and with low H-plane crosspolarization. The antenna also has the added advantage of being

compact in size and is designed to operate at IMT-2000 band.

2.1. Design Geometry

The basic geometry of the antenna element is shown in Figure 1 (a). The LIEH patch antenna integrates both the E- and H-shaped patch on the same radiating element. For the E-shaped, the slots are embedded in parallel on the radiating edge of the patch, symmetrically with respect to the centerline, while for the H-shaped the slots are embedded in serial on the non-radiating edge of the patch, symmetrically with respect to the centerline.

The design adopted the two-dielectric layers approach [13] with a low permittivity dielectric forming the superstrate supporting the inverted radiating element above a ground plane with an air-filled substrate sandwiched between them as shown in Figure 1 (b). An L-shape probe is employed for feeding the element [14].

The L-probe feeding technique with a thick air-filled substrate has been reported to enhance the antenna bandwidth [15-17], while inverted radiating patch offers gain enhancement and at the same time protects from the environment effect. Both techniques offer easy patch fabrications, especially for array structures. The use of parallel slots on the patch on the other hand improves crosspolarization while the introduction of series slots reduces the size of the patch [18-20].

Figure 1. (a) Top view, (b) Side view of the 4×1 LIEH shaped broadband microstrip array antenna

The LIEH patch was fabricated on Rogers RT 5880 with dielectric permittivity, ε_{rl} of 2.2 and with thickness, h_l of 1.5748 mm. The thickness of the air-filled substrate, h_0, is 16 mm. A light weight aluminum sheet ground plane with dimension of 200×180 mm and thickness of 1 mm is supported by screws of 3 mm diameter. Figure 2 shows the fabricated element and Table 1 gives the design specification of the patch.
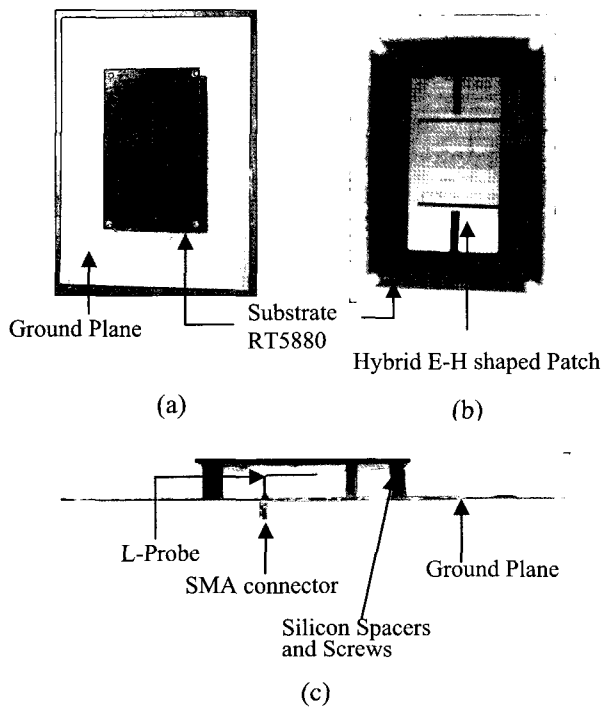

(a)   (b)

(c)

Figure 2.   (a) Top view, (b) E-H shaped patch and (c) Side view of the fabricated LIEH shaped patch antenna

Table 1. The inverted hybrid E-H shaped patch element design specification

Superstrate	RT 5880 (ε_{rl}=2.2, h_l=1.5748 mm)
Substrate	Air (ε_0=1, h_0=16 mm)
Rectangular patch	Width and Length, $\{W, L\}$=$\{79, 41\}$ mm
Feed Position	fp=8.5 mm from bottom edge of the patch
Slots parameters (E)	$\{ls, s, ws\}$ = $\{37, 16, 1\}$ mm
Slots parameters (H)	$\{lh, wh, sh\}$ = $\{18, 19, 2\}$ mm
Probe length	h_p=14 mm along y axis l_p=25 mm along x axis
Input impedance	50 Ω

3. ARRAY DESIGN

In an array antenna, multiple radiating elements are assembled in an electrical and geometrical configuration forming the antenna array. The amplitude and phase excitation (weight vectors) are adjusted at each individual radiating element to steer/form the beam to the intended user/target and placing null to the interferers. The antenna elements can be arranged in various geometries, such as linear, circular or planar. Uniform linear array is commonly used for horizontal beamforming and it gives sufficient performance for outdoor environment [21].

A broadband array antenna is needed in a smart antenna testbed to characterize the IMT-2000 or 3G radio specifications and performance evaluations. Special feeding schemes utilizing a group of power divider and wideband impedance matching technique using the coupled lines have been adopted by many researchers for the array development [10-11]. However, these techniques complicate the design procedure, especially if a large array structures are required. To ease the design procedure and make the system cost effective, a simple array system is required.

The following subsection discusses the design of a compact and broadband uniform linear array antenna for 3G base station based on the novel LIEH microstrip patch antenna discussed in Section 2. Due to the high cost and complexity of the design for planar and high resolution array, the design focuses on the development a four-element (4×1) array antenna. An L-probe fed feeding technique will be employed for the array similar to the single element design for easy of fabrication and integration at the base station.

3.1. Geometry of a LIEH Shaped Patch Antenna Array

The geometry of the 4×1 LIEH broadband microstrip array antenna is shown in Figure 3 (a). The array employed the inverted hybrid E-H element with the dimension of each element {W, L} = {79, 41} mm and with inter-element spacing of 68 mm (or 0.50λ) at 2.2 GHz. The total dimension of the array is 120 mm (width) by 285 mm (length) with the size of the ground plane equal to 370 mm × 200 mm × 1 mm.

The antenna array is fabricated on Rogers RT 5880 with dielectric permittivity, ε_{rl}, of 2.2 and with thickness h_l, of 1.5748 mm. The thickness of the air-filled substrate, h_0, is 16 mm. The array antenna employs four identical L-shaped probe feds of copper wire with a radius of 1 mm as shown in Figure 3 (b).

The horizontal and vertical dimensions of each probe are 25 mm and 14 mm, respectively. All the L-shaped probes are connected to the feed network, located underneath the ground plane via SMA connectors. The fabricated 4×1 LIEH broadband microstrip array antenna is shown in Figure 4.

(a)   (b)
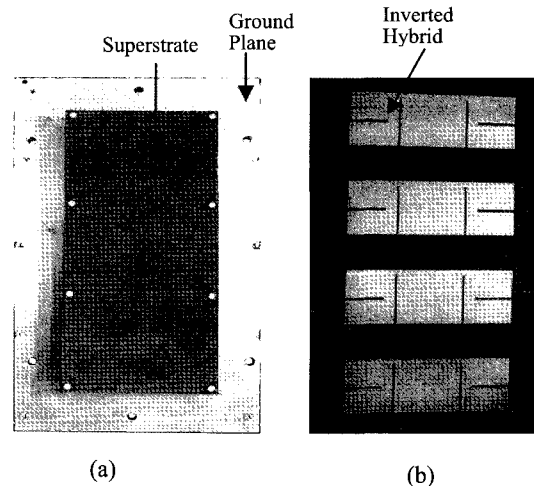
Figure 4. The fabricated 4×1 LIEH broadband microstrip array antenna (a) top view (b) inside view showing inverted elements.

(a)

(b)
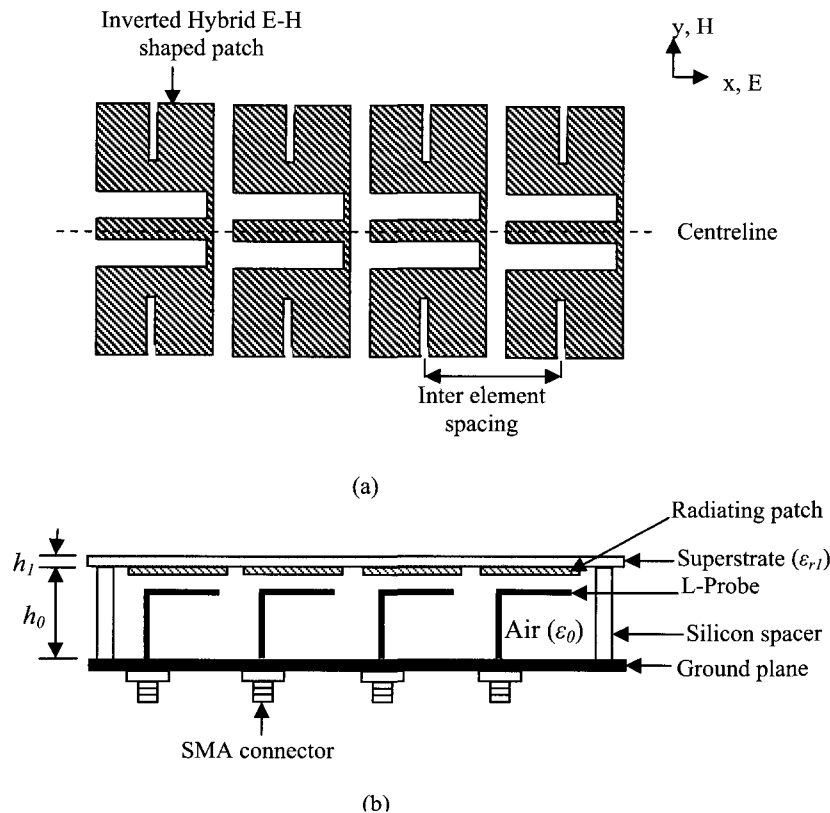
Figure 3. (a) Top view, (b) Side view of the 4×1 LIEH shaped broadband microstrip array antenna

3.2. Beamforming feed network

The beamforming feed network for the antenna array consists of a 4-way corporate structure Wilkinson power divider to feed the 4 antenna elements and a network of phase shifter-attenuator which is connected in series as shown in Figure 5. The phase shifter-attenuator network comprises of a commercial off-the-shelf variable phase shifter KPH350SC00 and step-rotary attenuator KATID04SA002, both from KMW Inc. The 4-way Wilkinson power divider was developed and fabricated in-house. Table 2 gives the summary of the beamforming feed network design and its electrical parameters.
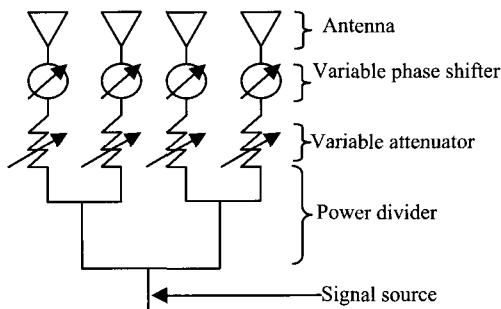
Figure 5. Schematic diagram of a beamforming feed network

Table 2. Summary of the beamforming feednetwork

A. Wilkinson Power Divider	
Substrate	Taconic RF-35 (ε_r=3.5, h=0.76 mm)
Bandwidth	460MHz (1.83-2.29GHz)
Return Loss	18.96dB (VSWR=1.25)
Isolation	19.77dB
Insertion loss	0.32dB
Amplitude Balance	0.70dB
Phase Balance	5.40°

B. Phase shifter	
Insertion loss	0.25dB (1-2GHz) 0.35dB (2-3GHz)
VSWR	1.25
Phase shift	35° @ 2GHz
C. Attenuator	
Frequency range	DC~3 GHz
Insertion loss	0.2dB
VSWR	1.15
Attenuation step	10 attenuation step of 1dB

Figure 6 shows the fabricated beamforming feed network connected to the antenna array. The power divider shown in this picture is covered by an aluminium shield and the antenna array is behind the power divider.
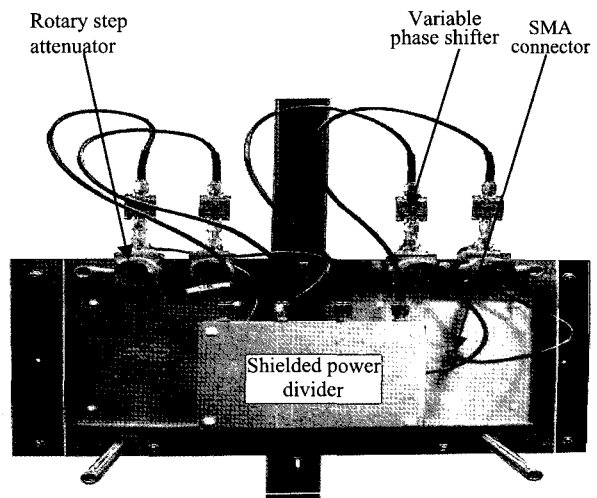

Figure 6. Rear view of the 4×1 LIEH broadband microstrip array antenna with a beamforming network.

4. RESULT AND DISCUSSIONS

The LIEH antenna element, the 4×1 antenna array, and the power divider were all fabricated

in-house. A commercial electromagnetic simulator *Sonnet® Suite em* simulator was used to simulate the design. The fabricated antennas and power divider were measured using the Agilent PNA E8358A network analyzer, Agilent ESG-DP series E4436B signal generator, Advantest R3131A spectrum analyzer, and the standard gain LPDA-0803 log periodic dipole antenna. Measurement was conducted in the open field.

4.1. LIEH Single Patch Antenna

4.1.1 Impedance Bandwidth

Figures 7 and 8 give the measured and simulated VSWR and Return Loss (RL) of the LIEH single patch antenna. The simulated and the measured results are in good agreement. Noted in both of these figures, the antenna resonates at 1.92GHz and at 2.15GHz where these closely excited

adjacent resonant frequencies resulted in a broadband characteristic of the antenna. These dual resonance frequencies are due to the effect introduced by the embedded parallel slots structure of the rectangular patch. As shown in Figure 8, the measured impedance bandwidth of 17.20% is obtained, covering the frequency range from 1.86-2.21GHz at 14dB return loss. Our designed antenna gave a slightly narrower bandwidth compared to the design demonstrated in [7-9]. This is due to the fact that our antenna is designed to give a better return loss by optimizing the slots to excite at a closer resonance frequencies, without sacrificing the bandwidth requirement of the IMT-2000 band.
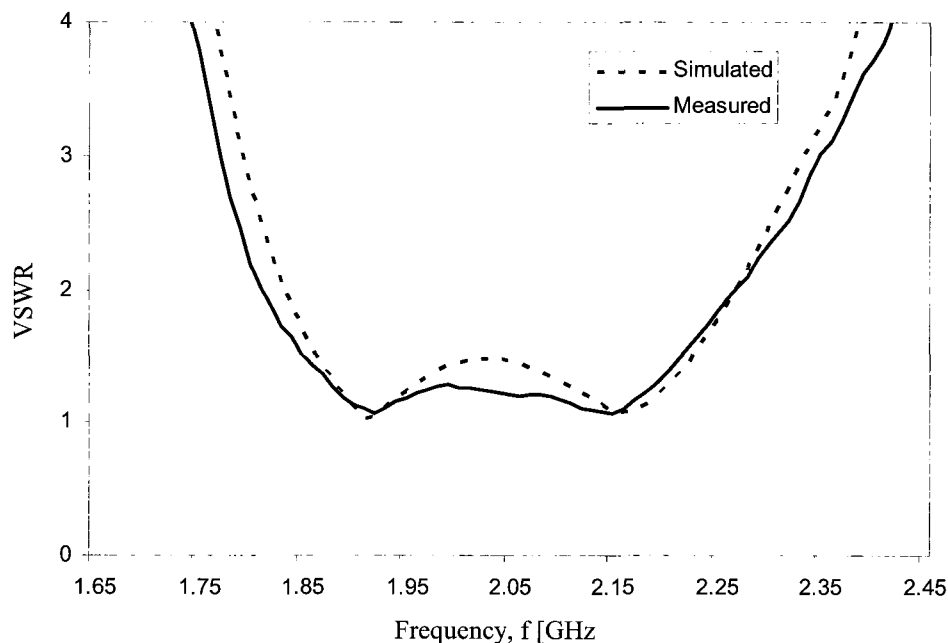

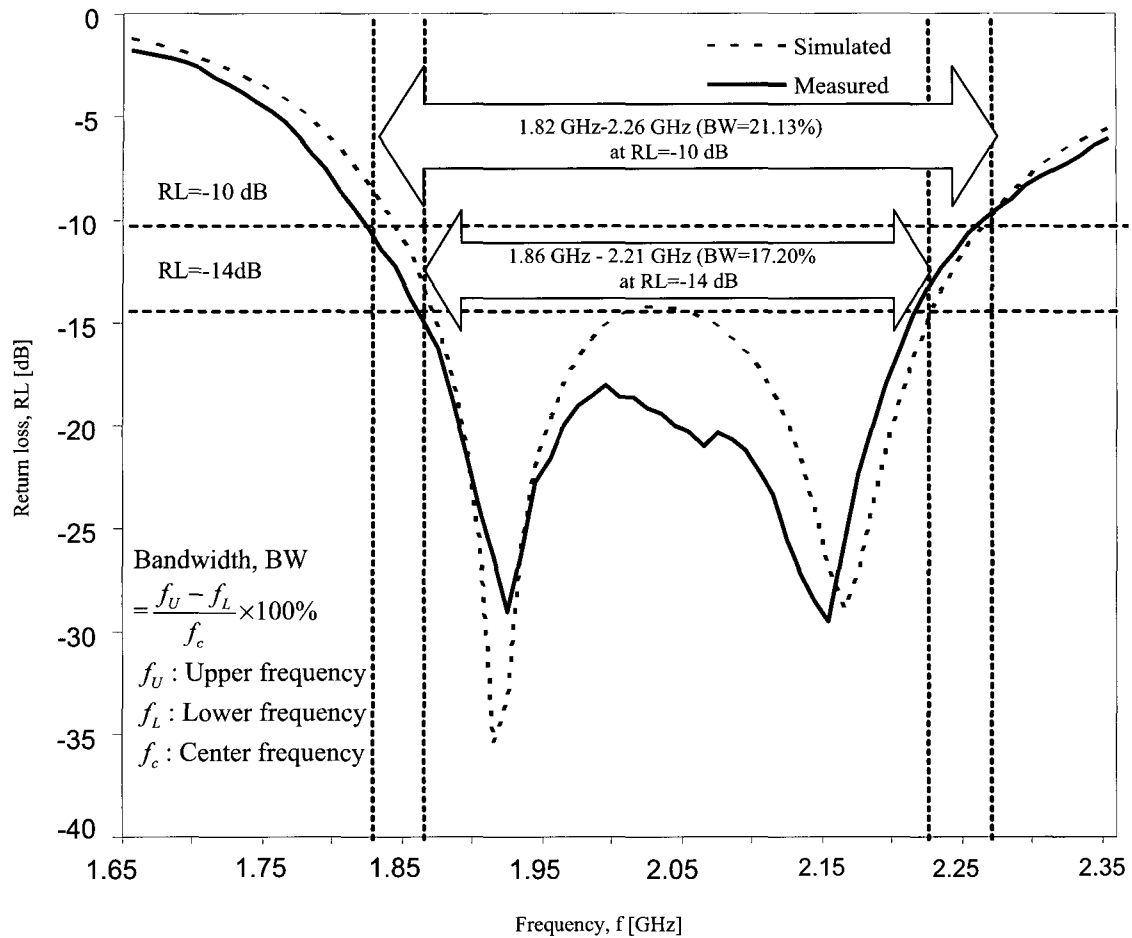Figure 7. Measured and simulated VSWR of the LIEH patch antenna

Figure 8. Measured and simulated Return Loss of the LIEH patch antenna.

4.1.2 Current Density

To comprehend the broadband and size reduction mechanism of the design LIEH patch antenna, the currents density of the antenna at both high and low resonance frequencies are investigated. For comparison, the current density for the L-probe inverted H-shaped patch antenna is also presented.

Figures 9 and 10 show the Sonnet® emvu current density for the L-probe H-shaped patch antenna and the inverted hybrid E-H microstrip antenna at both high and low frequencies. The label Jx and Jy on the figures represent the current flow in the E- and H-plane, respectively. As shown in the figures, it can be observed that strong current Jx flow along the L-probe on the patches and cover larger area

at high resonant frequency than at low resonant frequency. This larger area of currents Jx at high frequency can be modeled as additional capacitance. This additional capacitance results in additional higher resonant frequency that leads to the broadband characteristic of the patch if the two resonant frequencies are closely excited.

The introduction of series slots perturbed the current distribution on the patches as shown in the figures. For the H-shaped patch, strong current Jy are observed along the edge of the slots while strong current Jx are observed at the end of the slots at both high and low frequencies. These show that the current flows around the slots continuously with stronger current flow at low frequency. These strong current flows result in

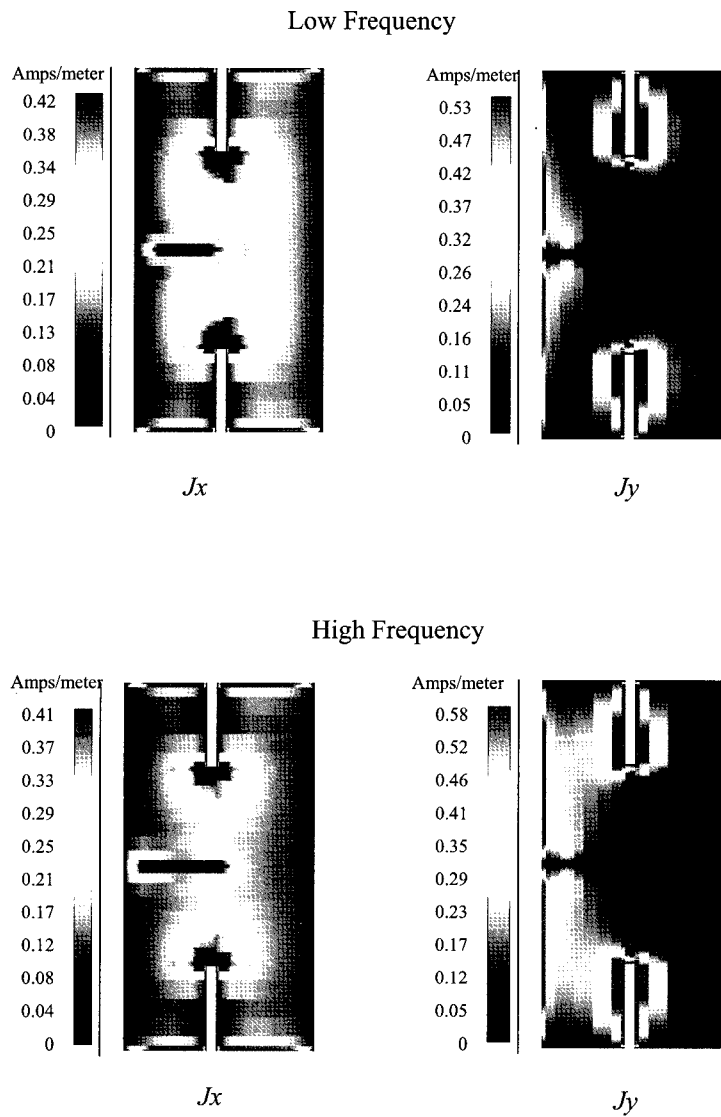longer electrical length of the patch hence reducing the patch length.

Low Frequency

Jx

Jy

High Frequency

Jx

Jy

Figure 9. The current density of L-probe fed H-shaped patch antenna at resonance frequencies. Colors on the patch represent amplitude/meter.

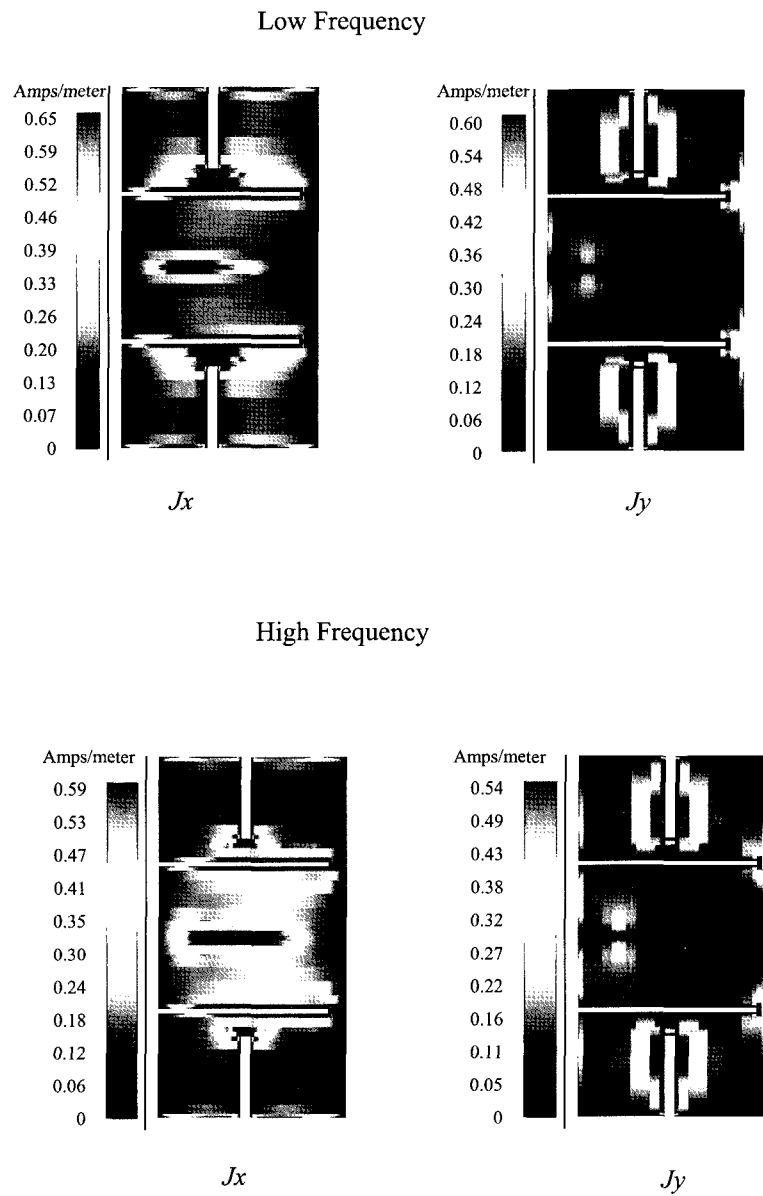Low Frequency

Jx Jy

High Frequency

Jx Jy

Figure 10. The current density of L-probe fed hybrid E-H shaped patch antenna at resonance frequencies. Colors on the patch represent amplitude/meter.

The addition of parallel slots on the patch forming the hybrid E-H shaped patch as shown in Figure 10 introduced favorable effect. Strong currents Jx are observed along the slots and strong currents Jy are observed at the end of the slots. From the figure, one can observe that currents Jx is greater than currents Jy indicates the basic cavity mode of the patch is TM_{10} mode. As shown in these Figures 9 and 10 Jy for the hybrid E-H patch is lower than Jy for the H-shaped and dramatically lower at high frequency for the hybrid E-H patch. Therefore, the inverted hybrid E-H microstrip patch antenna has lower crosspolarization level compared to the H-shaped patch. Such implication is mainly due to the introduction of additional parallel slots which obstruct the current flows in Jy direction from the center of the patch.

4.1.3 Radiation Pattern

The radiation characteristics of the LIEH patch antenna measured in free space range are shown in Figure 11. It shows the E-plane and H-plane radiation pattern of the hybrid patch at resonance frequency of 1.92GHz and 2.15GHz. The experimental results agree well with the simulation results (not shown in this paper). In the E-plane, the 3-dB beamwidth is 60° at 1.92GHz and 50° at 2.15GHz. The peak crosspolarization is -25dB at 1.91GHz and -30dB at 2.15GHz. The LIEH patch antenna shows that the crosspolarization level increases with resonant frequency and thickness [20]. The H-plane radiation pattern shows a slightly broader 3-dB beamwidth about 75°. The peak crosspolarization is -11.87dB and -9.82dB at the respected resonant frequencies. The improvement in the crosspolarization characteristics of the patch is due to the embedded parallel slot which reduces the current flow in H-plane direction as observed earlier. Noted in this

figure, the crosspolarization in the H-plane is considerably higher than the E-plane. Similar observations have been reported in the literature [7]. This crosspolarization is generated by the leaky radiation of the slots [7] and also due to the substrate thickness [22].
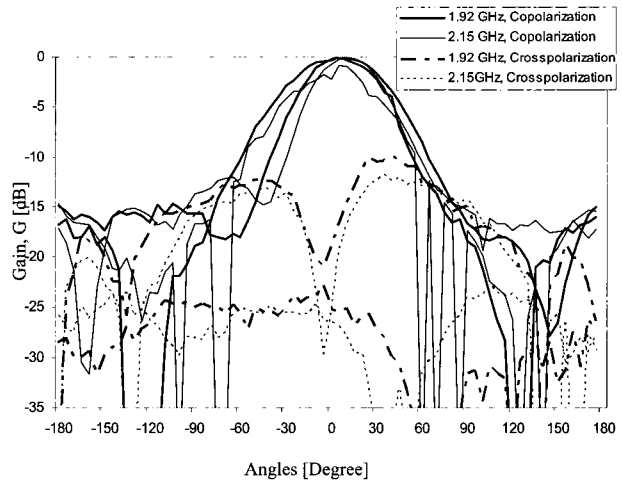

Figure 11. Measured E- and H-plane normalized radiation patterns at two resonant frequencies of 1.92GHz and 2.15 GHz.

4.2. LIEH 4×1 patch antenna array

4.2.1 Impedance bandwidth

Figures 12 and 13 show the measured input reflection coefficient S_{11} and VSWR of the first element of the array. The SWR is less than 2 in the frequency range from 1.80 to 2.24GHz equivalent to an impedance bandwidth of 21.78%. At SWR less than 1.5, the impedance bandwidth is 17.32% for the frequency range between 1.855 and 2.20GHz, wide enough to cover the IMT-2000 band. Other array element shows similar frequency dependence.
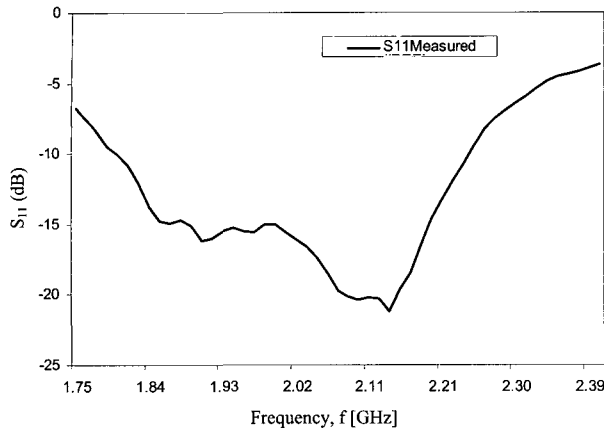
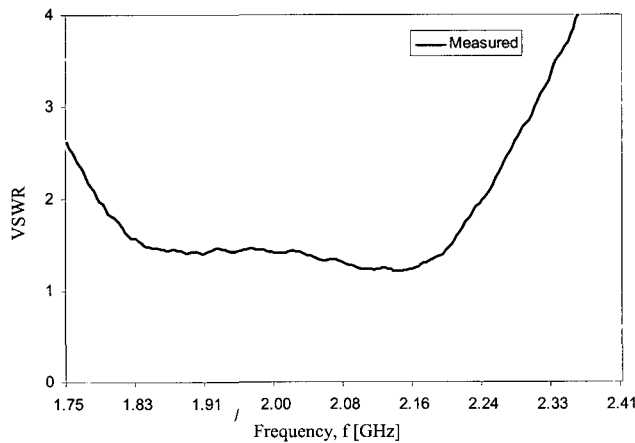Figure 12. Measured input reflection coefficient S_{11} of element-1.

Figure 13. Measured VSWR of element-1

4.2.2 Mutual Coupling

The impedance and radiation pattern of an antenna element changes when the element is radiating in the vicinity of other elements, this effect is known as mutual coupling. Consideration of mutual coupling is not required for a practical microstrip array, which has fixed beam at broadside (non-scanning arrays). However, the effects of mutual coupling can be detrimental on the array performance for microstrip array that has capability of scanning, using electrically thick substrate and with main beam far off broadside

[23]. Therefore, the design of microstrip antenna for smart antenna must include the mutual coupling into consideration.

Mutual coupling can be determined by observing the surface current distribution of the patch or by directly measuring the coupling between the elements (e.g. S_{12}, S_{13}, and S_{14}). Figure 14 shows the simulated patch's surface current distribution for the antenna array. The surface currents are obtained using *Sonnet em* with the cell size set at 1×1 mm, box size set to 902×691 cells, height of the free space set at 68 mm, and with maximum subsection set at 20 subsections per lambda. In this simulation, the element-1 is excited with voltage source of 1 volt at 1.91GHz. As shown in the figure, naturally, element-1 exhibits strongest current density, some current can be seen to couple to other element, but with reduced density as the elements are further spaced.
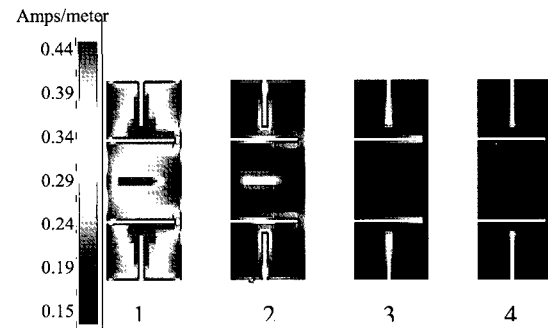

Figure 14. Current density for 4×1 LIEH patch array antenna at 1.91 GHz

Figure 15 shows the measured S_{12}, S_{13}, and S_{14} of the array with element-1 taken as the reference element. It can be seen that the coupling between the reference element and other elements decays over elements spacing. As shown in the figure, the magnitude of S_{12}, S_{13}, and S_{14} remains flat over the pass band and the maximum mutual coupling is between element-1 and element-2, S_{12}, with
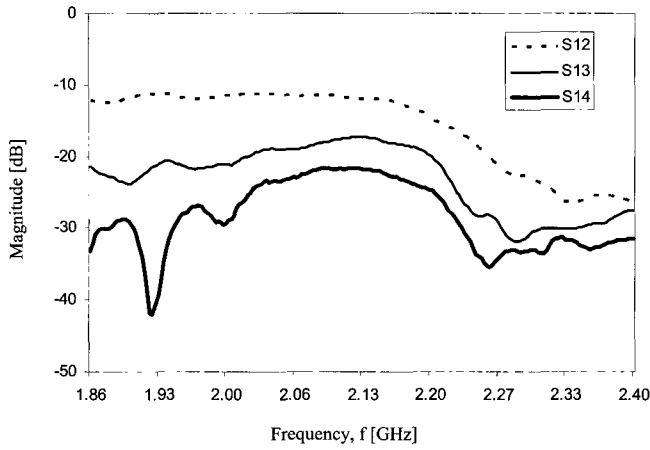
maximum value of -12.2dB in the operating bandwidth.

Figure 15. Measured coupling between element-1 and other elements of the LIEH patch array antenna

4.2.3 Radiation Pattern

Figures 16 and 17 show the E-plane and H-plane radiation patterns of the array antenna at 1.91GHz and 2.14GHz (resonance frequencies). The radiation patterns show some fluctuations due to the reflection from some obstacles in the field, however, they have good beam patterns and crosspolarization level. For the E-plane, the 3dB beamwidth are closed to 25° while for the H-plane the 3dB beamwidth is about 65°. The H-plane radiation pattern is virtually symmetry while the E-plane radiation pattern exhibits some asymmetries, similar to the report in [24] using a thick substrate. As shown in Figure 16, the sidelobe levels are unequally distributed. The first side lobe levels at 1.91GHz and 2.14GHz are 16.12 dB (at -60°) and -20.53 dB (at -95°) respectively. This result is due to the amplitude/phase unbalances in the beamforming feed network.
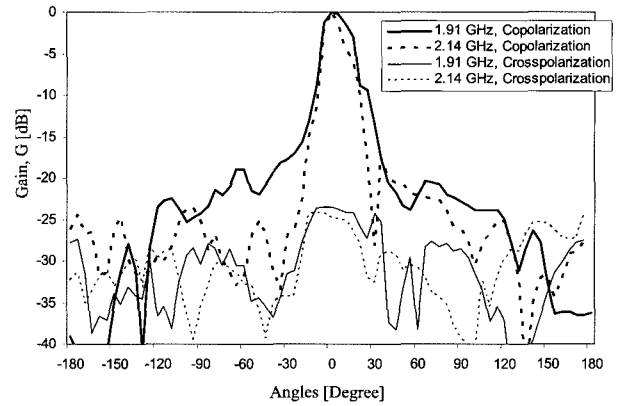

Figure 16. Measured E-plane normalized radiation patterns for the LIEH patch array antenna at 1.91GHz and 2.14 GHz.
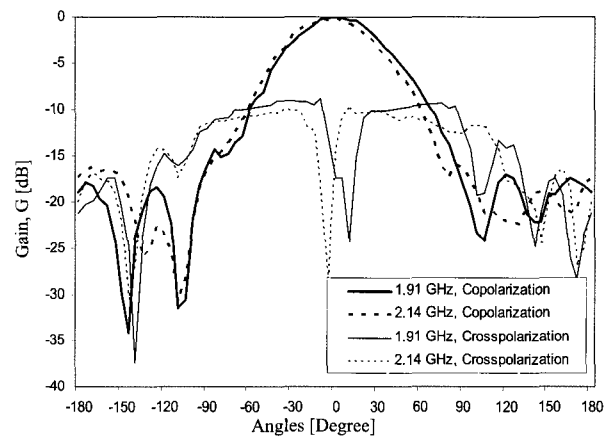

Figure 17. Measured H-plane normalized radiation patterns for the LIEH patch array antenna at 1.91GHz and 2.14GHz.

The maximum crosspolarization of the array is in the order of -21dB and -10dB in the E-plane and H-plane respectively. The maximum gain of the array is 11.9dBi. Figure 18 shows the radiation pattern of E-plane scanning at an angle of -10°. Here, the main beam is fixed at -10° measured from broad side, so the phase in each element of the array is progressively shifted by $\alpha=-\beta d\cos\theta$ =-153.48°, where β is the phase shift factor and d is the inter-element spacing. For this case, the peak

sidelobe level is about -13dB at 50°. The first side lobe level is -12.63 at 25°. The 3dB beamwidth is measured to be around 25° at both resonance frequencies. For -20° and -30° scanning first side lobe level is -11.68dB and -10.1dB, respectively (not shown in this paper).
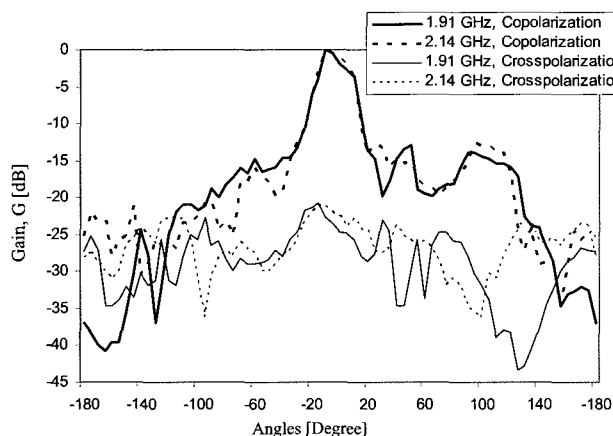

Figure 18. Radiation pattern of E-plane scanning at angle -10° for the LIEH patch array antenna

5. CONCLUSION

This paper discusses the design, development, and measurement of a broadband antenna array for smart antenna testbed for 3G base station using a novel broadband and compact inverted hybrid E-H microstrip patch with L-probe fed. Due to the high cost and complexity of the design for planar and high resolution array, the design focuses on the development of a uniform four-element (4×1) array antenna. The array design employed a novel LIEH shaped microstrip patch antenna element which provides better size reduction (22% reduction compared to the normal rectangular patch) and crosspolarization apart form the broadband features of the patch. The design of LIEH patch antenna is detailed in the paper. The array, with the elements spacing 0.5λ, provides an impedance bandwidth of 440MHz or about 21.78% at 10dB return loss, referenced to the center frequency at 2.02GHz and the mutual coupling is about 12dB between the first two elements of the array. The crosspolarization radiation in the E-plane patterns of the array is about -21dB and -10 dB for the H-plane. The beamforming feed network was constructed using a four-way Wilkinson power divider of corporate structure type and a phase shifter-attenuator networks, connected in series to the ports to examine the scanning capability of the array.

The array developed and fabricated in-house has been shown to function well within its design ability. However, further development is necessary to allow for two-dimensional scanning and with higher scanning resolution. The use of a programmable phase shifter-attenuator and a DSP controller would enhance the capability of the beamforming feed network and to bring the intelligence to the antenna, hence, functioning as a smart antenna. The use of higher elements array and with proper pattern synthesis could enhance the performance of the array by reducing the side-lobe level to the acceptable level. Improved patch design would give better broadband and compactness of the array. The arrays find application for smart antenna systems in the 3G cellular communication.

ACKNOWLEDGMENTS

REFERENCES

[1] F. Adachi, M. Sawahashi, and H. Suda, "Wideband DS-CDMA for next generation mobile communication systems," *IEEE Commun. Magazine,* vol. 36, no. 9, pp. 56-59, 1998.

[2] S. Choi, and D. Shim, "Correction to a novel adaptive beamforming algorithm for a smart antenna system in a CDMA mobile communication environment," *IEEE Trans. on Vehicular Technology,* vol. 51, no. 6, pp. 1671 – 1672, 2002.

[3] S. Ohmori, Y. Yamao, and N. Nakajima, "The future generations of mobile communications based on broadband access technologies," *IEEE Commun. Magazine,* vol. 38, no. 12, pp. 134 – 142, 2000.

[4] P. E. Mogensen, F. Frederiksen, H. Dam, K. Olesen, and S. L. Larsen, "TSUNAMI II stand-alone testbed," *Proc. of ACTS Mobile Summit,* Granada, Spain, pp. 517-527, 1996.

[5] J. Monot, J. T. Hibault, P. Chevalier, F. Pippon, and S. Mayrague, "Smart antenna prototype for the SDMA experimentation in UMTS and GSM/DCS 1800 network," *Proc. of PIMCR-97, IEEE,* Helsinki, Finland, pp. 333-337, 1997.

[6] R. B. Ertel, Antenna array systems: propagation and performance, PhD Thesis, Virginia Polytechnic Institute and State University, 1999.

[7] T. Huynh, and K. F. Lee, "Single-layer single-patch wideband microstrip antenna," *IEEE Electron. Lett.* vol. 31, no.16, pp. 1310-1312, 1995.

[8] K. F. Lee, K. M. Luk, K. F. Tong, S. M. Shum, T. Hunh, and R. Q. Lee, "Experimental and simulation studies of the coaxially fed U-slot rectangular patch antenna," *Proc. Inst. Elect.* *Eng. Microw. Antennas Propagat.,* vol. 144, no. 5, pp. 354-358, 1997.

[9] K. L. Wong, and W. H. Hsu, "A broad-band rectangular patch antenna with a pair wide slits," *IEEE Trans. on Antennas Propagation,* vol. 49, no. 9, pp. 1345-1347, 2001.

[10] Y. An, L. Xin, and G. Benqing, "Developing a kind of microstrip array antenna with beam squint," *Proc. of 5th Intern. Symposium on Antennas, Propagation and EM Theory, ISAPE 2000, IEEE,* pp. 443 – 446, 2000.

[11] K. I. Jeong, and Y. J. Yoon, "Design of wideband microstrip array antennas using the coupled lines," *IEEE Intern. Symposium on Antennas and Propagation Society,* vol. 3, pp.1410-1413, 2000.

[12] K. M. Luk, K. F. Lee, and W. L. Tam, "Circular U-slot patch with dielectric superstrate," *IEEE Electron. Lett.* vol. 33, no. 12, pp. 1001-1002, 1997.

[13] K. J. Ng , Z. A. Abdul Rashid, and M. T. Islam, "Broadband inverted E-shaped rectangular microstrip patch antennas for 3G applications," *IEEE Natl. Symposium on Microelectronics, NSM-2003,* Perlis, Malaysia, pp. 286-289, 2003.

[14] K. J. Ng, Design and development of broadband microstrip antenna for 3G wireless network, MSc Thesis, University Kebangsaan Malaysia, 2004.

[15] C. L. Mak, K. F. Lee, and K. M. Luk, "Microstrip line-fed L-strip patch antenna," *IEE Proc. Microwaves, Antennas and Propagation* vol. 146, no. 4, pp. 282-284, 1999.

[16] C. L. Mak, and K. M. Luk, "Experimental study of a microstrip patch antenna with an L-shaped probe," *IEEE Trans. on Antennas*

and Propagation, vol. 48, no.5, pp. 777- 783, 2000.

[17] Y. X. Guo, C. L. Mak, and K. M. Luk, "Analysis and design of L-probe proximity fed-patch antennas," *IEEE Trans. on Antennas and Propagation,* vol. 49, no. 2, pp. 145- 149, 2001.

[18] C. S. Hong, "Gain-enhanced broadband microstrip antenna," *Proc. of Natl. Sci. Counc. ROC (A),* vol. 23, no. 5, pp. 609-611, 1999.

[19] V. Palanisamy, and R. Garg, "Rectangular ring and H-shaped microstrip antennas-alternatives to rectangular patch antenna," *IEEE Electron. Lett.* vol. 21, no.19, pp. 874-876, 1985.

[20] S. C. Gao, L. W. Li, M. S. Leong, and T. S. Yeo, "A novel dual-polarized, wide-band microstrip patch antenna with aperture coupling," *IEEE Intern. Symposium Antennas and Propagation Society,* vol. 4, pp. 78-81, 2001.

[21] P. H. Lehne, and M. Pettersen, "An overview of smart antenna technology for mobile communication system," *IEEE Commun. Survey,* vol. 2, no. 4, pp. 14-23, 1999.

[22] T. Huynh, K. F. Lee, and R. Q. Lee, "Crosspolarization characteristic rectangular patch antennas," *IEEE Electron. Lett.* vol. 24, pp. 463-464, 1998.

[23] K. F. Lee, and W. Chen, eds., *Advances in Microstrip and Printed Antennas,* NJ, John Wiley & Sons, pp. 223-271, 1997.

[24] Chang, S. Long, and W. F. Richards, "An experimental investigation of electrically thick rectangular microstrip antennas," *IEEE Trans. on Antennas and Propagation,* vol. 34, no. 6, pp. 767 – 772, 1986.

Biography

Zainol Abidin Abdul Rashid is a lecturer at the Department of Electrical, Electronic and System Engineering, Faculty of Engineering, Universiti Kebangsaan Malaysia, Malaysia where he joined in 1989. He received his B.Sc. degree in Electronics from the same university in 1985 and obtained his M.Sc. degree in Microprocessor Engineering and PhD degree in Electrical Engineering from University of Bradford, UK in 1987 and 1997 respectively. He research into ice crystal crosspolarization effect on earth-satellite link at 20 GHz from the ESA Olympus satellite during his PhD work. After finishing his PhD work, he was appointed as a team leader for the first Malaysian microsatellite, TiungSAT-1. He is currently pursuing research in 3G air interface and smart antenna system, and leading the Malaysian team for the polar ionospheric and water vapour research at Scott Base, Antarctica. He is also involved in the development of aircraft collision avoidance system.

Mohammad Tariqul Islam was born in Dhaka, Bangladesh in 1975. He received his B.Sc. and M. Sc. Degree in Applied Physics and Electronics from University of Dhaka, Dhaka, Bangladesh in 1998 and 2000, respectively. He worked as a lecturer at International Islamic University Chittagong (IIUC), Dhaka. He is currently pursuing his PhD at Electrical, Electronics and System Engineering department at University Kebangsaan Malaysia with the supervision Dr. Zainol Abidin Abdul Rashid. His research interest includes Smart antenna system.

Liew Chang Sheng (no picture available) was born in Penang, Malaysia in 1980. He is pursuing his Bachelor Degree at Electrical, Electronics and System Engineering department at University Kebangsaan Malaysia with the supervision Dr. Zainol Abidin Abdul Rashid. He received his B.E. Degree in Communication and Computer in 2005. He now currently worked as a Design Engineer at Intel, Penang.